scientific reports

Check for updates

OPEN

Study on combustion reaction products and free radicals of aliphatic hydrocarbon functional groups in coal based on ML potential MD

Jinzhang Jia[1,2], Yumo Wu[1,2]✉, Dan Zhao[3], Fengxiao Wang[1,2], Dongming Wang[1,2], Qiang Yang[1,2] & Yinghuan Xing[1,2]

The Gas-phase products generated by aliphatic hydrocarbon functional groups during the spontaneous combustion of coal represent a significant source of environmental pollution. A primary focus of contemporary research is the investigation of their microscopic reaction pathways and the dynamics of free radical transformations. This study examines the combustion and pyrolysis reaction mechanisms of three distinct aliphatic hydrocarbon functional groups utilising the Machine Learning Potential Molecular Dynamics (ML potential MD) method, with validation conducted through thermogravimetric-Fourier transform infrared spectroscopy (TG-FTIR) and in-situ FTIR experiments. The findings suggest that the reactivity of the –CH group is the highest, followed by $–CH_2$, while $–CH_3$ exhibits the greatest stability. The –CH functional group exhibits the highest tendency for CH_4 produced, the $–CH_2$ group displays the highest tendency for CO_2 produced, and the $–CH_3$ group demonstrates the highest tendency for H_2O and CO produced. The ·O radical plays a pivotal role in promoting combustion in the oxidative combustion of functional groups, while both the ·HO radical and the ·H radical act as key initiators in this process. These findings offer theoretical insights into mitigating carbon emissions from the perspective of functional groups and free radicals.

Keywords Aliphatic hydrocarbon, Coal spontaneous combustion, Free radicals, Gas-phase products, ML potential MD

Coal has historically constituted the primary energy source in China. It is therefore of the utmost importance to ensure the efficient and safe development of this resource in order to guarantee national energy security and a stable supply[1,2]. However, during the processes of coal mining, storage and utilisation, instances of spontaneous combustion occur intermittently, resulting in the release of considerable quantities of toxic and harmful gases. Such occurrences not only result in the wastage of resources but also pose a significant threat to both the safety of production and the environmental integrity of the surrounding area. Consequently, these security risks are increasingly regarded as fundamental indicators for evaluating energy competitiveness[3]. The primary source of heat for spontaneous combustion in coal is aliphatic hydrocarbon functional groups[4]. It is therefore imperative to investigate the microscopic reaction pathways and mechanisms of these functional groups within coal in order to elucidate the underlying processes of coal spontaneous combustion. This research not only facilitates the scientific management of the coal development and utilisation process, but also contributes to the realisation of carbon neutrality and the advancement of sustainable development[5,6].

The extant research indicates that the spontaneous combustion of coal is significantly influenced by the presence of active aliphatic hydrocarbon functional groups within the coal matrix. The gas-phase products and free radicals generated during the combustion process have been the subject of considerable attention in industrial applications[7,8]. Chao et al.[9]employed gas chromatography to investigate the correlation between oxygen consumption rates and Gas-phase products, including CO_2 and CO, under conditions involving stress-

[1]College of Safety Science and Engineering, Liaoning Technical University, Fuxin Liaoning 123000, China. [2]Key Laboratory of Thermal Dynamic Disaster Prevention and Control of Ministry of Education, Liaoning Technical University, Huludao Liaoning 125105, China. [3]Faculty of Civil Engineering and Architecture, Zhanjiang University of Science and Technology, Zhanjiang 524000, Guangdong, China. ✉email: 13614067811@163.com

heat-gas interactions. The research results provide a theoretical basis for combating the spontaneous combustion of coal in complex coal mines. Duan et al.[10] investigated the reaction mechanisms of free radicals in coal spontaneous combustion by integrating electron spin resonance (ESR) and spin trapping techniques. The results demonstrated that coal consistently displays a high concentration of free radicals within the temperature range of 30 °C to 300 °C. It is noteworthy that an increase in the initial free radical content of coal samples correlates with elevated heating temperatures, thereby facilitating the conversion of these radicals. Tao et al.[11] employed electron spin resonance (ESR) technology to investigate the trends in free radical concentration, g-factor values, line width, and line shape in coal. The effects of varying oxidation times and oxygen concentrations on these free radical parameters were examined. The findings indicate that the relationship between free radical reactions and oxidation time is nonlinear, with oxygen molecules enhancing the reactivity of free radicals. The interaction of oxygen atoms with carbon chains results in the generation of both oxygen-containing free radicals and peroxide radicals. These subsequently decompose and oxidise into CO_2 and CO, which ultimately lead to the spontaneous combustion of coal. This methodology offers a novel perspective for analysing the roles of functional groups and free radicals during spontaneous combustion processes. However, it remains challenging to experimentally observe microscopic bond fractures as well as the formation of intermediates and free radicals.

Free radical reaction plays a crucial role in the process of coal spontaneous combustion, but there is still considerable scope for research on its fundamental reaction pathways and details. With the advent of sophisticated computational technology and software, researchers have largely turned to molecular dynamics (MD) methods to investigate free radicals, yielding notable insights[12,13]. Chen et al.[14] employed quantum chemical methods to elucidate the reaction pathways of free radicals during the spontaneous combustion of coal and introduced a novel cyclic model for these species within this context. It has been demonstrated that the majority of reactions involving free radicals are exothermic. In a recent study, Yan et al.[15] employed ReaxFF molecular dynamics simulations to investigate the influence of hydroxyl radicals on the reactivity of aromatic rings and their associated side chain functional groups.Their findings revealed that ·OH radicals played a crucial role in the formation of phenolic hydroxyl structures, subsequently catalyzing low-temperature coal oxidation processes. This discovery holds significant implications for the heat storage phase during low-temperature oxidation of coal. In another study employing ReaxFF MD simulations, Yan et al.[16] identified intermediate products corresponding to four distinct formation pathways, including CO_2. These results validated the precision of reaction molecular dynamics calculations and enhanced our understanding of CO_2 generation during coal combustion. Additionally, Zhang et al.[17] conducted quantum chemical calculations using Gaussian software to elucidate the microscopic mechanisms underlying alkane pyrolysis within oil shale kerogen molecules, thereby addressing certain limitations posed by experimental conditions.

As previously discussed, the molecular dynamics method is a powerful tool for investigating the microscopic mechanisms of free radicals and gas-phase products in coal spontaneous combustion reactions. However, variations in research methodologies and the limited training datasets have led to differing perspectives on the construction methods and rationality of molecular models[18,19]. Recently, Chi[20] introduced a machine learning force field in 2022 that leverages an extensive structural relaxation database. This advancement holds significant potential for applications in structural relaxation, dynamic simulations, and property predictions across diverse chemical spaces. In this study, we conducted the first ML potential MD simulation of the combustion reactions involving three aliphatic hydrocarbon functional groups using AMS(Amsterdam Modeling Suite)-2024 software. The model was validated through TG-FTIR and in-situ FTIR experiments. By analyzing changes in potential energy, consumption patterns of functional groups, variations in oxygen utilization, generation trends of gas-phase products, fluctuations in free radicals, and typical chemical equations associated with combustion reaction pathways, we elucidate the mechanisms by which functional groups influence coal's spontaneous combustion characteristics. This research provides theoretical insights for mitigating carbon emissions from a functional group perspective and offers novel avenues for developing inhibitors.

Modelling and simulation methods

Molecular models

Spontaneous combustion of coal is a complex reaction process that is predominantly influenced by the presence of various active functional groups within the coal structure. Among these, aliphatic hydrocarbon functional groups are regarded as the principal initial heat source for the coal-oxygen composite reaction[21,22]. In consequence of the above, three structural models of aliphatic hydrocarbon functional groups within coal were established using benzene rings as skeletal linkages[23], and molecular dynamics simulations were conducted to investigate the combustion reactions of $-CH_3$, $-CH_2$, and $-CH$. The initial step involved the construction of a periodic reaction box using the ML potential force field available in AMS-2024 software. This was done with the incorporation of 20 model compounds representing various functional groups.Subsequently, a specific quantity of O_2 molecules was introduced, and the dimensions of the periodic reaction box were adjusted for different reaction systems while maintaining a system density of 0.5 g/ml (with $a = b = c$). In order to achieve a balanced and stable initial structure, it is essential to allow the reaction system to relax. The M3GNet-UP-2022 parametric model was employed for this relaxation process. The periodic symmetry was configured as Bulk, and NHC temperature control was selected with a damping constant set at 10 K/fs, resulting in a total of 10,000 steps with a time step of 0.25 fs. The energy minimisation relaxation was conducted at an ambient temperature of 50 K[24]. The methodology employed for the construction of functional group structural models, along with the results obtained from relaxation studies, are illustrated in Fig. 1.

The potential energy curves of each structural model exhibited a gradual stabilization following an initial sharp decline. The structural models corresponding to each functional group were confined within the periodic reaction box, demonstrating stability without the emergence of new reactions. This observation indicates that a

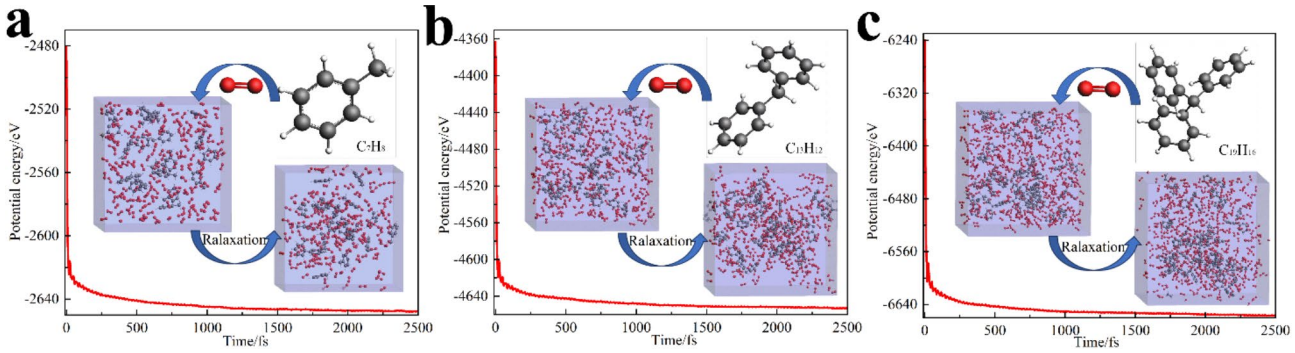

Fig. 1. Construction of functional group molecular model. (**a**) Relaxation analysis of -CH_3; (**b**) -CH_2; (**c**) Relaxation analysis of -CH_3.

balanced and uniform reaction system was achieved post-relaxation, with the reaction force field appropriately adapted to this system.

Molecular simulation methods

In order to elucidate the mechanism of oxygen compound reactions, combustion reaction systems were constructed for three aliphatic hydrocarbon functional group structure models under varying oxygen concentrations. The number of O_2 molecules consumed in the complete reaction for each functional group was determined through stoichiometric calculations, representing a complete combustion system with an equivalence ratio of (1) Subsequently, the O_2 concentration was doubled to establish an oxygen-rich combustion system with an equivalence ratio of (2) In parallel, oxygen-poor combustion systems with equivalence ratios of 0.75, 0.5, and 0.25 were created alongside a pyrolysis reaction system characterised by an equivalence ratio of 0, which served as the control group for comparison. Following the relaxation processes, it is essential to reset the reaction parameters for all three aliphatic hydrocarbon functional group structure models. Following relaxation, the three kinds of aliphatic hydrocarbon functional group structure model must also be reset with regard to the reaction parameters. The model selected was NVT system synthesis[25], with a total of 120,000 steps in the synthesis. The temperature interval was set at 298–2500 K-3500 K–400 K. The number of steps in the temperature range of 0–298 K is 10,000, 40,000, 60,000, and 10,000, respectively, with a step length of 0.25 fs. The damping constant is 10 K/fs, and NHC is selected for temperature control. The MD Properties module facilitated monitoring and capturing products generated during combustion reactions; subsequently allowing analysis on product distribution and elementary reactions.

Theoretical calculation methods

In the calculation of the bond interaction e_{ij}, it is essential for the structural model to account for all other bonds emanating from atom i. To effectively incorporate n-body interactions, each e_{ij} is updated by considering all distinct combinations of $n-2$ neighboring atoms (i.e., those in $N_{i/j}$) within Ni, excluding atom j[20]. This process can generally be expressed as follows:

$$\widetilde{e}_{ij} = \sum_{\substack{K_1,K_2,\cdots,K_{n-2}\in N_i/j \\ K_1!=K_2!=\cdots K_{n-2}}} \phi_n\left(e_{ij}, r_{ij}, v_j, r_{ik_1}, r_{ik_2}, \cdots, r_{ik_{n-2}}, v_{k_1}, v_{k_2}, \cdots, v_{kn_{n-2}}\right) \tag{1}$$

Where ϕ_n is the update function, r_{ij} is the vector from atom i to atom k, and v_{kI}, v_{k1} is the atomic information of atom k_1. The material map can be effectively modeled as MnGNet through a neural network that incorporates n-body interactions. This study will specifically concentrate on integrating three-body interactions, hence termed M3GNet.

The 'ML potential MD' simulation is governed by the system's potential energy, eliminating the need for a pre-defined reaction pathway. This approach can be broadly applied to various systems exhibiting complex chemical reactions, including combustion, oxidation, and pyrolysis of coal. The energy function of the system is expressed in the following form[26]:

$$E_{system} = E_{bond} + E_{lp} + E_{over} + E_{under} + E_{val} + E_{pen} + E_{tors} + E_{conj} + E_{vdwaals} + E_{coulomb} \tag{2}$$

Where E_{system} is the total energy of the system, E_{bond} is the bond energy, E_{lp} is the energy of long pair electrons, E_{over} and E_{under} are the correction term for coordination energy, E_{val} is the valence angle term, E_{pen} is the penalty energy, E_{tors} is the torsion energy, E_{conj} is the conjugation effects to molecular energy, $E_{vdwaals}$ is the non-bonded van der waals interaction, and $E_{coulomb}$ is the coulomb interaction. Among them[27] :

$$E_{bond} = -D_e^{\sigma} BO_{ij}^{\sigma} \exp\left[p_{be1}\left(1-\left(BO_{ij}^{\sigma}\right)^{p_{be2}}\right)\right] - D_e^{\pi} BO_{ij}^{\pi} - D_e^{\pi\pi} BO_{ij}^{\pi\pi} \tag{3}$$

where D_e^{σ},D_e^{π} and $D_e^{\pi\pi}$ are the force field parameters of single, double and triple bond related to bond energy, $p_{be1}$and p_{be2} are temporary parameters, Furthermore[28]:

$$BO'_{ij} = BO_{ij}^{\sigma} + BO_{ij}^{\pi} + BO_{ij}^{\pi\pi} = \exp\left[p_{bo1}\left(\frac{r_{ij}}{r_0^{\sigma}}\right)^{p_{bo2}}\right] + \exp\left[p_{bo3}\left(\frac{r_{ij}}{r_0^{\pi}}\right)^{p_{bo4}}\right] + \exp\left[p_{bo1}\left(\frac{r_{ij}}{r_0^{\pi\pi}}\right)^{p_{bo6}}\right] \quad (4)$$

where BO'_{ij} is the bond order between atoms i and j, r_{ij} denotes the distance between atoms and r_0 are the equilibrium bond length for bonds σ, π and ππ.

Experimental parameter settings

Coal preparation

In this study, the long-flame coal sourced from the Heidaigou Open-pit Coal Mine in Inner Mongolia was selected as the experimental sample. The large coal specimens extracted on-site were securely wrapped in nitrogen-filled plastic to facilitate transport to the laboratory. To prevent oxidation, the outer layer of each coal specimen was removed, and the inner fresh coal was subsequently crushed and sieved to a particle size of 200 mesh[29,30]. Initially, the coal samples were dried at room temperature for 24 h before undergoing industrial elemental analysis. The results are presented in Table 1. The experimental coal samples exhibited elevated carbon (C) content, oxygen (O) content, and volatile matter levels, rendering them susceptible to spontaneous combustion under identical conditions.

TG-FTIR experiment

The TG instrument utilized was the Netzsch 209F3 from Germany, while the FTIR spectrometer employed was the Bruker TENSOR27, also from Germany. The TG-FTIR combined experiment enables simultaneous acquisition of data regarding changes in coal sample quality parameters and the infrared spectra of gaseous product content at varying temperatures. The carrier gas was air (V_{O_2}:V_{N_2} = 1/4), the temperature was set at 30 ~ 800 °C, the temperature increase rate was set at 10 K/min, the resolution of the infrared spectra was 4 cm^{-1}, the number of scans was 32, and the range of the tested wave numbers was 600 ~ 4000 cm^{-1} in the mid-infrared. Specific absorption peaks were monitored for H_2O at 3735 cm^{-1}, CO_2 at 2359 cm^{-1}, CO at 2120 cm^{-1}, and CH_4 at 3016 cm^{-1}[31]. The diversity of gas phase products is influenced by temperature, as shown in Fig. 2 (a).

In-situ FTIR experiment

The in-situ FTIR instrument employed is the German Bruker VERTEX 80v. The carrier gas utilized is air, with a flow rate set at 50 ml/min. A total of 32 scans were conducted, achieving a resolution of 4 cm^{-1} and covering a spectral range from 600 to 4000 cm^{-1}. The experimental temperature was maintained between 30 °C and 300 °C, with a heating rate of 10 K/min; data points were collected at intervals of every 2 °C[32,33], as shown in Fig. 2(c).

Validate simulation results

To validate the rationality of the simulation results, a comparison is made between these results and experimental findings. The TG-FTIR experiment provides a temporal sequence of gas-phase product formation during the heating process of coal samples. The obtained data are juxtaposed with the temporal sequence of gas-phase products from three aliphatic hydrocarbon functional groups in the simulation, as shown in Fig. 2(b). The analysis reveals that the order of gas-phase products generated during heating is: $H_2O > CO_2 > CO > CH_4$, demonstrating consistency between simulation outcomes and experimental observations. In the In-situ FTIR experiment, a lower consumption of functional groups with increasing temperature indicates greater stability of the functional group structure. Similarly, in the simulation results, an extended duration for the consumption of functional groups as temperature rises correlates with enhanced structural stability. A comparative analysis of these findings, as shown in Fig. 2(d). The data demonstrate that the order of structural stability among the three oxygen-containing functional groups, ranked from weakest to strongest, is as follows: -CH < $-CH_2$ < $-CH_3$; Notably, these simulation outcomes align well with those obtained from in-situ FTIR experiments. Therefore, this provides evidence to support the validity of both the simulation methodology and the parameter settings employed in this study.

Results and discussion

Analysis of combustion reaction behavior of aliphatic hydrocarbon functional groups

Evolution process of combustion reaction system

Currently, capturing the microstructural changes occurring during the combustion process of materials through experimental research poses significant challenges[28]. Consequently, this study simulates and investigates the microstructure of three aliphatic hydrocarbon functional groups in coal throughout the heating process. Using a complete combustion reaction system with an oxygen content equivalence ratio of 1 as a case study, visual representations of these three functional groups at various time intervals are presented in Fig. 3. The combustion

Proximate analysis/%			Ultimate analysis/%				
Moisture on an air-dried basis(M_{ad})	Ash on a dry basis(A_{ad})	Volatile matter on a dry and ash-free basis(V_{ad})	C	H	O	N	S
2.79	23.30	27.93	76.98	4.94	12.26	1.39	0.33

Table 1. Proximate Analysis and Ultimate Analysis of long-flame coal.

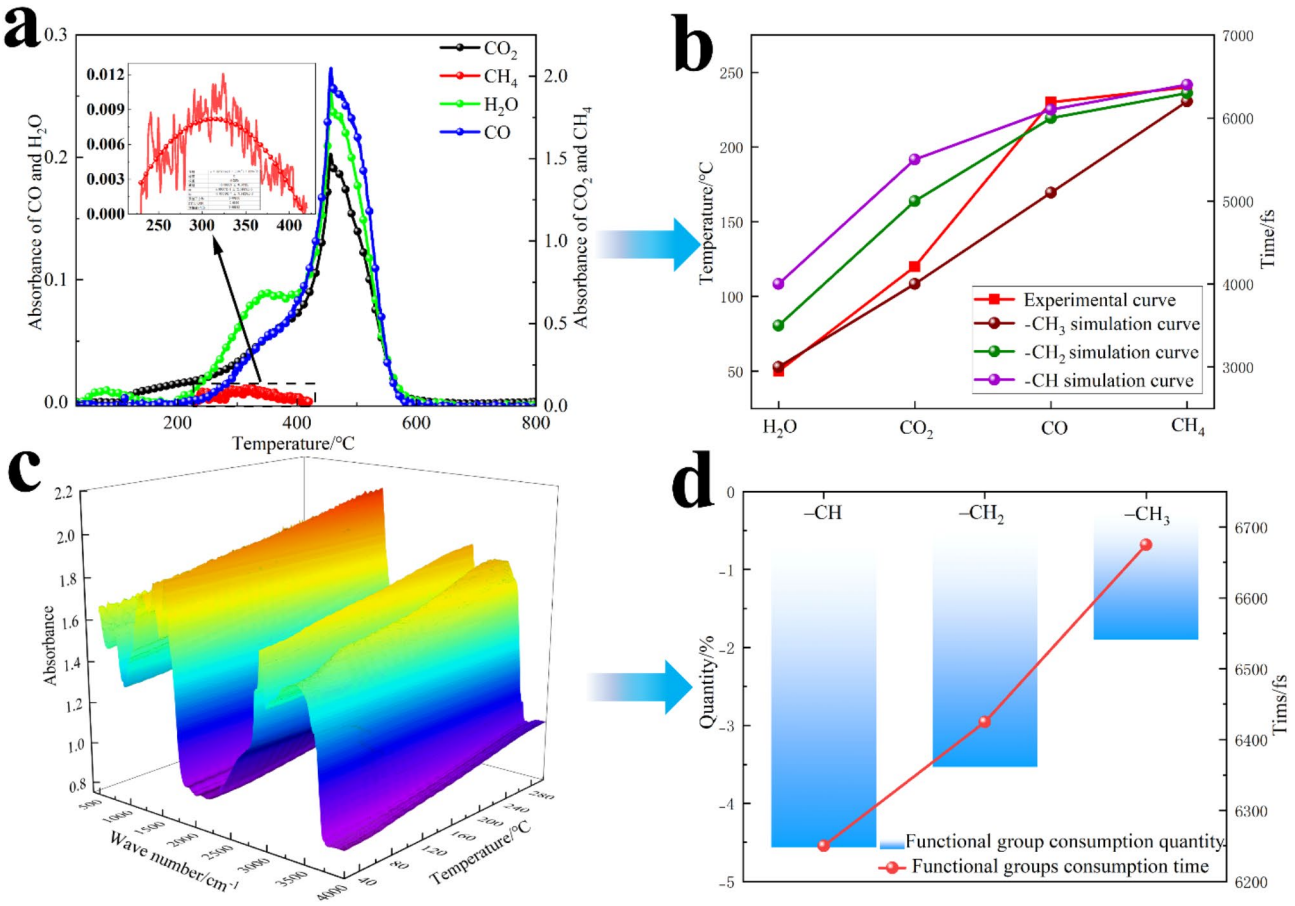

Fig. 2. Comparison between simulation and experiment. (**a**) Distribution law of gas phase products of long-flame coal in air atmosphere; (**b**) Comparison of gas phase product distribution between simulation and experiment. (**c**) In-situ 3d infrared map of long-flame coal in air atmosphere; (**d**) Comparison of functional groups consumption between simulation and experiment.

reaction process of each functional group can be delineated into four distinct stages: the first stage, known as the pre-reaction stage (0 ~ 2500 fs), primarily involves the diffusion of functional groups and O_2 molecules; the second stage encompasses the oxidation combustion reaction stage (2500 ~ 12500 fs), during which the system increasingly exhibits characteristics indicative of vigorous combustion reactions. The third stage is characterized as a continuous reaction stage (12500 ~ 27500 fs), wherein oxidation reactions involving carbon-containing molecular fragments and the formation and consumption of free radicals predominate, resulting in substantial gas-phase products release. The fourth stage represents the completion of reactions (27500 ~ 30000 fs), allowing for oscillation and diffusion within molecular structures to maintain uniformity in internal distribution, thereby facilitating observation and analysis of reaction outcomes. Notably, significant physical and chemical transformations within the system occur predominantly during both the oxidation combustion reaction phase and continuous reaction phase; thus, these two stages are emphasized in this paper for an in-depth analysis of the evolution process within functional group combustion systems.

Potential energy

The potential energy graphically depicts the heat absorption and release of each functional group model reaction system, where a downward-sloping curve indicates a heat-releasing system and an upward-sloping curve represents a heat-absorbing system. Notably, higher potential energy correlates with lower stored energy, thereby reducing the energy required for the thermal decomposition of functional groups. The potential energy changes of the three aliphatic hydrocarbon functional groups under different oxygen content conditions are shown in Fig. 4 (a ~ c). It can be observed that the heat uptake and exothermic patterns of the three functional aliphatic hydrocarbon energy groups demonstrate a consistent trend under the reaction system with varying oxygen contents. In the pre-reaction stage, the potential energy curves exhibit an upward trajectory, and the system rapidly absorbs heat with the increase of temperature, reaching the preset temperature required for the reaction. From the outset of the oxidative combustion reaction stage, the potential energy curves exhibited a downward trajectory in both the oxygen-enriched and complete combustion reaction systems, indicative of a robust exothermic reaction. Conversely, in oxygen-deficient systems, a reduction in oxygen content leads to insufficient availability of reactants required for subsequent oxidation reactions; consequently, the potential energy curve

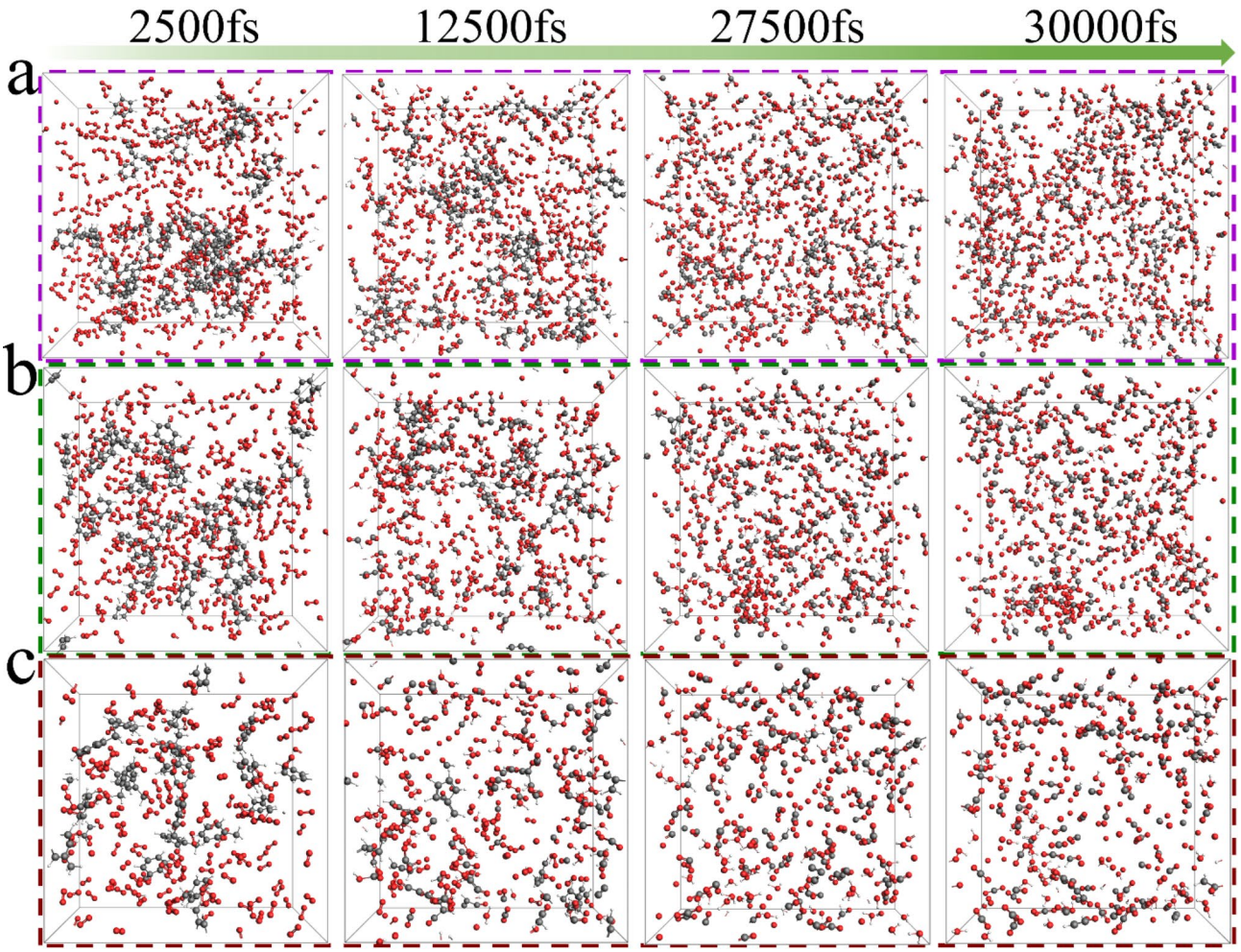

Fig. 3. The evolution process of complete combustion reaction system with different functional groups. (**a**) -CH; (**b**) $-CH_2$; (**c**) $-CH_3$.

gradually trends upwards. This behavior signifies an endothermic state where lower oxygen levels precipitate earlier occurrences of endothermic reactions. Under anaerobic pyrolysis conditions, potential energy curves display a consistent upward trajectory, suggesting that anaerobic pyrolysis of aliphatic hydrocarbon functional groups is inherently endothermic. The initial exothermic and subsequent endothermic behaviors observed in functional groups within oxygen-poor environments further substantiate from a molecular perspective that actual spontaneous coal combustion processes are frequently accompanied by parallel phenomena such as coal pyrolysis.

Quantity of O2

The combustion reaction pathways of functional groups represent a complex process of oxidation reactions. O_2 serves as a crucial promoter for these combustion reactions, playing an essential role in facilitating combustion and sustaining the oxidation processes of the functional groups. Consequently, investigating the oxygen consumption patterns of three distinct functional groups under varying oxygen concentrations is vital for enhancing our understanding of the oxidation reaction pathways among these groups. The O_2 consumption patterns observed in the combustion reaction systems involving these three functional groups at different oxygen levels, as shown in Fig. 4 (d ~ f). The temporal variation in oxygen consumption across the three functional groups under different oxygen content reaction systems exhibits a notable consistency. Specifically, an increase in O_2 concentration within the reaction system correlates with an extended duration for oxygen consumption. In scenarios where the O_2 content corresponds to a complete combustion reaction system with an equivalence ratio of 1, each functional group's reaction system depletes all available O_2 before reaching 27,500 fs, thereby validating the appropriateness of the O_2 levels established for complete combustion across these three functional groups. Conversely, at an equivalence ratio of 2, the oxygen consumption observed in the three functional group reaction systems surpasses that of the complete combustion scenario; furthermore, their respective oxygen consumption curves exhibit a gradual decline. This indicates that when sufficient O_2 is present along with adequate time and spatial conditions for reactions to occur, oxidation processes involving transition products generated during

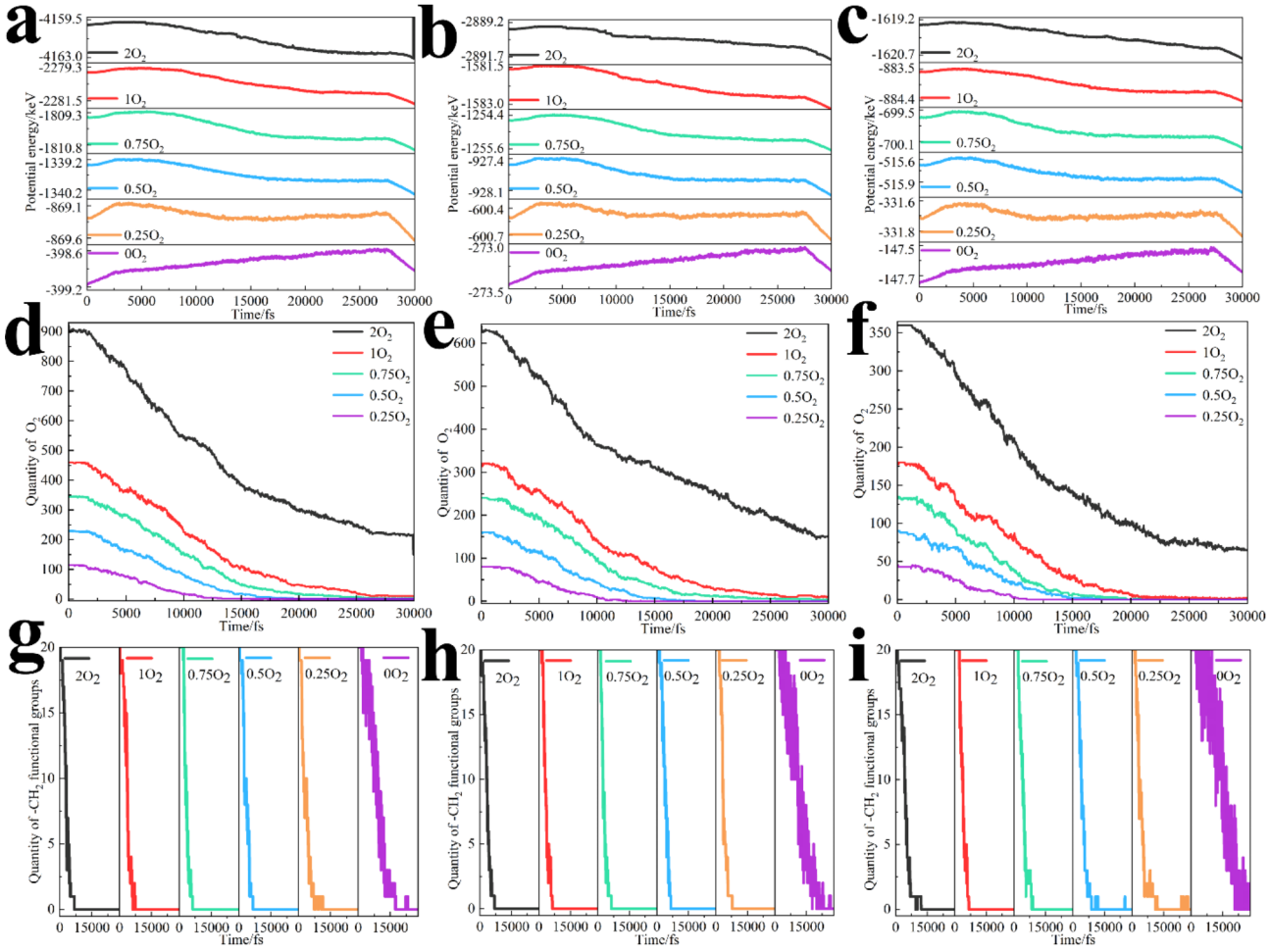

Fig. 4. Analysis of combustion reaction process of different functional groups. (**a**) Potential energy analysis of -CH; (**b**) $-CH_2$; (**c**) $-CH_3$. (**a**) Analysis of oxygen consumption of -CH; (**b**) $-CH_2$; (**c**) $-CH_3$. (**a**) Consumption analysis of -CH; (**b**) $-CH_2$; (**c**) $-CH_3$.

combustion are enhanced significantly. This extension of oxidative chain reactions further underscores that oxidation-combustion represents a complex reactive process.

Quantity of functional groups

The structural decomposition times of three oxygen-containing functional group model compounds attached to the benzene ring vary with temperature due to differences in their functional group structures. Consequently, the timing of changes in the conjugate system of these functional groups serves as an indicator for assessing the order of combustion consumption completion among the three aliphatic hydrocarbon functional groups. Additionally, this timing can also provide insights into the stability of these groups[34]. As shown in Fig. 4(g ~ i), the completion time for −CH consumption is 6250 fs, while that for CH_2 and CH_3 are 6425 fs and 6675 fs, respectively. Thus, we can infer a stability hierarchy within the combustion reaction system: $-CH < -CH_2 < -CH_3$. The typical reaction path snapshots of the combustion processes involving three aliphatic hydrocarbon functional groups, as shown in Fig. 5, where the shadow background indicates the critical path for the change of the functional group conjugate system. The spontaneous combustion of coal is a very complex process that may also involve reactions of the singlet-biradical characters in long PAHs with molecular oxygen[35]. Through an analysis of the molecular dynamics simulation trajectory, we elucidate the microstructural transformations and decomposition pathways of these functional groups. The intermediate products predominantly manifest as cycloalkanes, cycloolefins, and their isomers. It becomes evident that the fundamental nature of the oxidative combustion reaction pathway for aliphatic hydrocarbon functional groups lies in the oxidative dehydrogenation effect exerted by these functional groups. This mechanism generates carbon-containing fragments and various free radicals that facilitate subsequent oxidation reactions involving the functional groups. Furthermore, peroxides and complexes formed during this oxidative dehydrogenation process contribute to heat accumulation, thereby promoting further progression of the combustion reaction. Among these, $-CH_3$ features three carbon-carbon σ bonds, which are carbon-hydrogen bonds directly linked to the carbon atoms and exhibit the highest structural stability. In contrast, $-CH_2$ possesses one carbon-carbon σ bond and one carbon-carbon π bond, rendering it unsaturated and relatively unstable. Meanwhile, −CH contains a single carbon-carbon triple bond, also classified

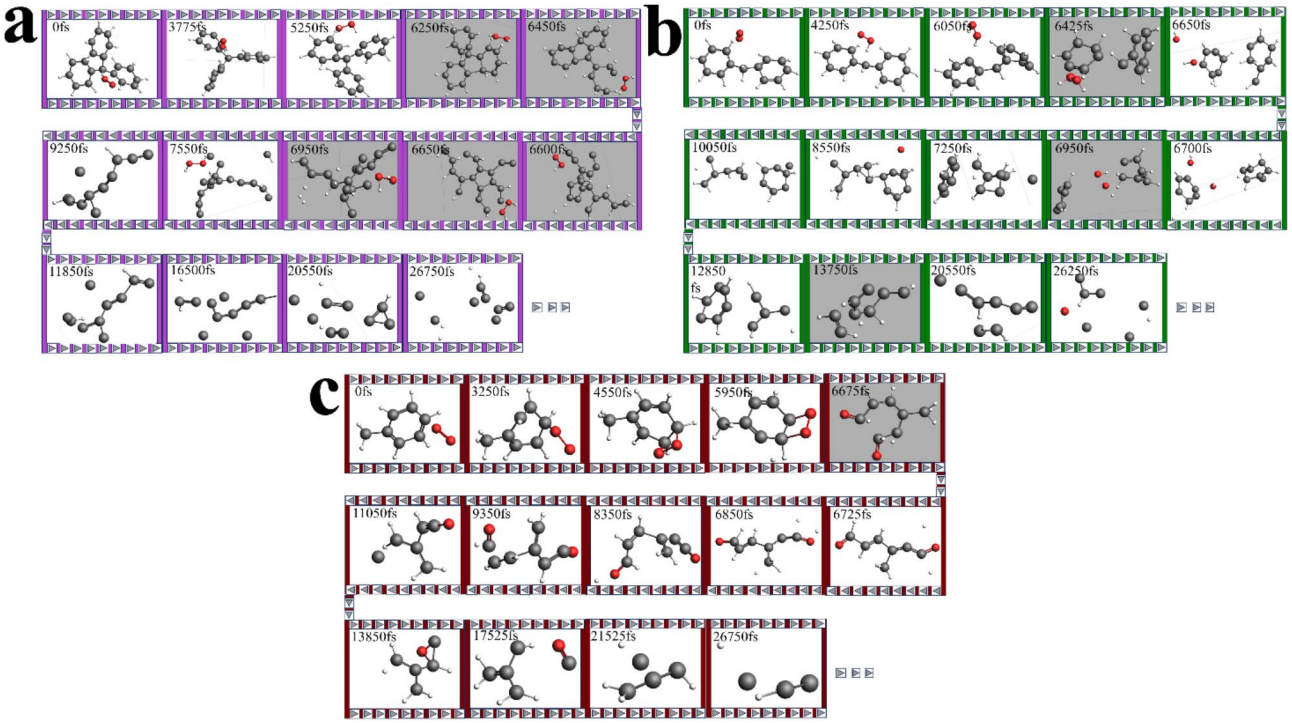

Fig. 5. Typical reaction path snapshots of combustion of different functional groups. (**a**) -CH; (**b**) $-CH_2$; (**c**) $-CH_3$.

as unsaturated, making it more reactive and thus the most unstable of the three. Consequently, due to the distinct structures of these three aliphatic hydrocarbon functional groups, their respective conjugated systems undergo different transformations. In the $-CH_3$ system, the oxidation reaction preferentially disrupts the benzene ring by targeting its π electron cloud, leading to the degradation of the conjugated system. Conversely, in the $-CH_2$ system, it is primarily the unsaturated bond between two benzene rings that undergoes cleavage before subsequent ring-opening occurs. In contrast, within the −CH system, recombination of both benzene rings takes precedence, resulting in a five-membered cyclopentane structure. This preference arises from the inherent stability of five-membered rings due to their lower internal strain; thus, formation of this intermediate effectively reduces the overall energy of the system and drives the reaction in this direction. Consequently, energy within this context predominantly facilitates ring-opening processes in benzene rings, culminating in a more readily disrupted conjugated system associated with −CH.

Analysis of combustion reaction products of aliphatic hydrocarbon functional groups

The combustion and pyrolysis of coal can generate thousands of hydrocarbons. In this paper, only the major ones (CH_4, H_2O, CO, CO_2) are reported. The Gas-phase products resulting from the functional groups of aliphatic hydrocarbon primarily consist of H_2O, CO_2, and CO. The quantities of these three Gas-phase products fluctuate over time under varying oxygen content reaction systems, as shown in Fig. 6. Additionally, the representative chemical equations for the formation pathways of these three Gas-phase products are presented in Table 2. The three gas-phase products began to emerge gradually during the oxidative combustion stage of the functional groups, with their production significantly increasing in the continuous reaction phase. Notably, H_2O is formed first, traceable to the onset of the reaction. Analyzing the typical chemical equation for H_2O formation reveals that aliphatic hydrocarbon functional groups initiate this process. The generation of H_2O is accompanied by numerous consumption reactions predominantly occurring in the mid-to-late stages of the combustion reaction system involving functional groups. This transformation involves converting thermal decomposition reactions of H_2O molecules into free radicals and is highly influenced by temperature; it represents a classic exothermic reaction. The formation of CO_2 occurs later than that of H_2O. In the initial stages of aliphatic hydrocarbon functional group reactions, there are fewer pathways available for the oxidation of carbon-containing products to yield CO_2. The generation of CO_2 primarily results from reactions between small molecular fragments with low carbon content and free radicals. This process is exothermic, and the resultant gas contributes to the release of combustion energy. After 5000 fs, all three aliphatic hydrocarbon functional groups begin to produce CO, with its formation occurring subsequent to that of both CO_2 and H_2O. The formation pathway of carbon monoxide necessitates that oxygen radicals engage in an oxidative pre-reaction with carbonaceous fragments. The energy associated with the chemical bonds formed during these reactions exceeds that of the broken bonds, indicating that this process requires energy absorption to proceed, characteristic of a typical endothermic reaction. The consumption pathway of CO predominantly occurs during the continuous reaction phase involving functional

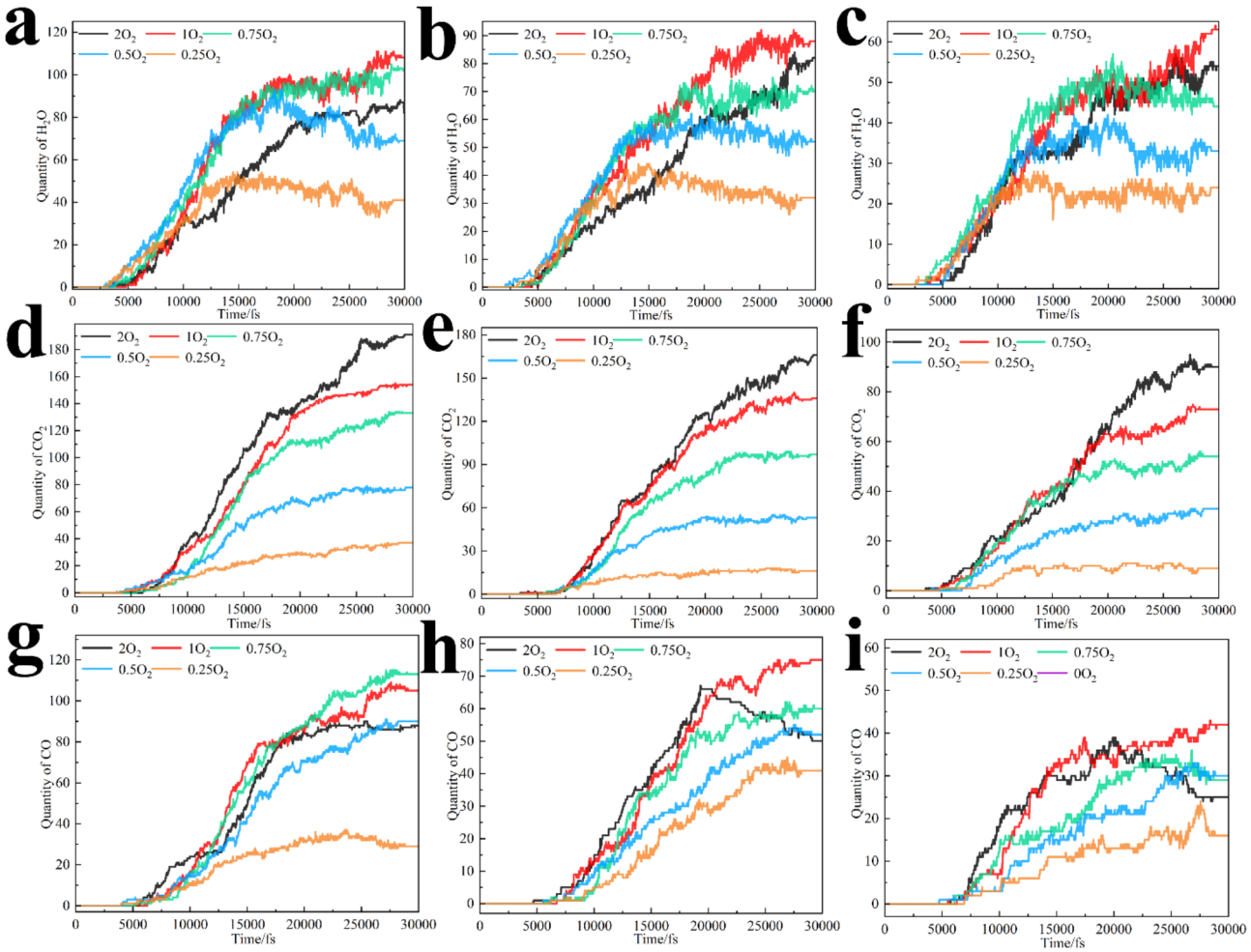

Fig. 6. Analysis of combustion reaction products of different functional groups. (**a**) H_2O production of -CH; (**b**) $-CH_2$; (**c**) $-CH_3$. (**d**) CO_2 production of -CH; (**e**) $-CH_2$; (**f**) $-CH_3$. (**g**) CO production of -CH; (**h**) $-CH_2$; (**i**) $-CH_3$.

groups. This process entails the combustion of CO to produce CO_2 at elevated temperatures, representing a quintessential oxidative exothermic reaction.

The impact of oxygen content on the three gas products varies significantly. In an oxygen-enriched combustion reaction system with an O_2 equivalence ratio of 2, the production of H_2O is lower than that observed in a complete combustion reaction system with an O_2 equivalence ratio of 1, This observation aligns with the trends indicated by the consumption curves of the three functional groups, suggesting that the inhibitory effect of the oxygen-enriched system on the combustion reactions involving these functional groups primarily manifests through dehydrogenation processes and alterations in ·HO radical conversion pathways. Furthermore, higher O_2 concentrations in other reaction systems correlate with increased H_2O production. Aliphatic hydrocarbon functional groups show consistency in CO_2 production under different oxygen content reaction systems, that is, the higher the O_2 content in the reaction system, the more CO_2 is produced.The oxygen-enriched combustion environment exerts a significant inhibitory effect on the formation of CO from aliphatic hydrocarbon functional groups. This phenomenon can be attributed to the preferential oxidation of these functional groups into oxygen-containing small molecular compounds prior to CO formation. From this analysis, it is evident that the dynamics within an oxygen-enriched combustion system are profoundly influenced by spatial interactions. The increase of the reaction pathway facilitates the conversion of a greater quantity of carbonaceous fragments into CO_2 at elevated conversion rates, thereby resulting in a reduction in CO production. In comparison to other Gas-phase products, the formation pathway of CO is significantly influenced by O_2 concentration and the nature of functional groups. As illustrated in Table 2, variations in ·O free radicals exert a substantial impact on the formation pathways of both CO_2 and CO. Notably, there exists a positive correlation between ·O free radical concentrations and CO_2 production, while an inverse relationship is observed with respect to CO production. Furthermore, fluctuations in ·HO radicals markedly affect the formation pathway of H_2O, demonstrating a positive correlation between these two factors.

H_2O	CO_2	CO
$\cdot HO + C_{19}H_{16} => H_2O + C_{19}H_{15}$	$\cdot H + C_{19}H_{10}O_5 => CO_2 + C_{18}H_{11}O_3$	$C_{19}H_{12}O_5 => CO + C_{18}H_{12}O_4$
$\cdot HO + C_{13}H_{12} => H_2O + C_{13}H_{10}$	$C_{18}H_{10}O_5 => CO_2 + C_{17}H_{10}O_3$	$C_{18}H_8O_5 => CO + C_{17}H_8O_4$
$\cdot HO + C_7H_8 => \cdot H + H_2O + C_7H_6$	$C_{17}H_5O_9 => CO_2 + C_{16}H_5O_7$	$C_{17}H_4O_{10} => CO + \cdot H + C_{16}H_3O_9$
$\cdot H + \cdot HO + C_{18}H_{10}O_3 => H_2O + C_{18}H_{10}O_3$	$C_{16}H_4O_8 => CO_2 + C_{15}H_4O_6$	$C_{16}H_6O_{10} => CO + C_{15}H_6O_9$
$\cdot HO + C_{16}H_5O_8 => H_2O + C_{16}H_4O_8$	$C_{15}H_3O_9 => CO_2 + C_{14}H_3O_7$	$C_{15}H_5O_5 => CO + C_{14}H_5O_4$
$\cdot HO + C_{15}H_6O_5 => H_2O + C_{15}H_5O_5$	$C_{14}H_4O_9 => CO_2 + C_{13}H_4O_7$	$C_{14}H_4O_6 => CO + C_{13}H_4O_5$
$\cdot HO + C_{14}H_6O_4 => H_2O + C_{14}H_5O_4$	$C_{13}H_8O_3 => CO_2 + \cdot H + C_{12}H_7O$	$C_{13}H_8O_3 => CO + C_{12}H_8O_2$
$\cdot HO + C_{12}H_6O_5 => H_2O + C_{12}H_5O_5$	$\cdot H + C_{12}H_3O_5 => CO_2 + C_{11}H_4O_3$	$C_{12}H_7O_3 => CO + C_{11}H_7O_2$
$\cdot HO + C_{11}H_3O_2 => H_2O + C_{11}H_2O_2$	$C_{11}H_5O_5 => CO_2 + C_{10}H_5O_3$	$C_{11}H_3O_7 => CO + C_{10}H_3O_6$
$\cdot HO + C_{10}H_3O_3 => H_2O + C_{10}H_2O_3$	$C_{10}H_4O_5 => CO_2 + C_9H_4O_3$	$C_{10}H_3O_5 => CO + C_9H_3O_4$
$\cdot HO + C_9H_5O_3 => H_2O + C_9H_4O_3$	$C_9H_5O_3 => CO_2 + C_8H_5O$	$C_9H_3O_4 => CO + C_8H_3O_3$
$\cdot HO + C_8H_4O => H_2O + C_8H_3O$	$C_8H_3O_2 => CO_2 + C_7H_3$	$C_8H_2O_3 => CO + C_7H_2O_2$
$\cdot HO + C_6H_6O => H_2O + C_6H_5O$	$C_7H_4O_2 => CO_2 + C_6H_4$	$C_7H_4O_5 => CO + C_6H_4O_4$
$\cdot HO + C_5H_5O_5 => H_2O + C_5H_4O_5$	$C_6H_4O_4 => CO_2 + C_5H_4O_2$	$C_6H_3O_3 => CO + C_5H_3O_2$
$\cdot HO + C_4H_2O_4 => H_2O + C_4HO_4$	$C_5H_2O_2 => CO_2 + C_4H_2$	$C_5H_3O_4 => CO + C_4H_3O_3$
$\cdot HO + C_3H_2O => H_2O + C_3HO$	$C_4H_2O_3 => CO_2 + C_3H_2O$	$C_4H_2O_3 => CO + C_3H_2O_2$
$\cdot HO + C_2H_5O_2 => H_2O + C_2H_4O_2$	$C_3HO_3 => CO_2 + C_2HO$	$C_3HO_3 => CO + C_2HO_2$
$\cdot HO + CH_2O_3 => H_2O + CHO_3$	$C_2HO_4 => CO_2 + \cdot CHO_2$	$C_2HO_4 => CO + \cdot HO + CO_2$
$\cdot HO + \cdot H => H_2O$	$\cdot CHO_2 => CO_2 + \cdot H$	$\cdot CHO + \cdot HO => CO + H_2O$
$H_2O => \cdot HO + \cdot H$	$CO + \cdot CHO_2 => CO_2 + \cdot CHO$	$CO + \cdot O => CO_2$

Table 2. Typical chemical equations of gas phase product formation reaction path. The gas-phase product serves as a crucial indicator for assessing the combustion reaction process. The conversion rate of gas-phase products can be utilized to evaluate the conversion tendencies across various functional group reaction systems. Specifically, a higher conversion rate of a gas phase product indicates a more pronounced tendency for conversion within the combustion reaction system's functional groups. The formula for calculating the gas-phase product conversion rate is as follows:

$$\eta_{H_2O} = \frac{N_{H_2O}}{N_H} \tag{5}$$

where η_{H_2O} is H_2O conversion rate (%), N_{H_2O} is the number of H_2O molecules produced, N_H is the number of H atoms of the functional group.

$$\eta_{CO_2} = \frac{N_{CO_2}}{N_C} \tag{6}$$

where η_{CO_2} is CO_2 conversion rate (%), N_{CO_2} is the number of CO_2 molecules produced, N_C is the number of C atoms of the functional group.

$$\eta_{CO} = \frac{N_{CO}}{N_C} \tag{7}$$

where η_{CO} is CO conversion rate (%), N_{CO} is the number of CO molecules produced.

Using the complete combustion reaction system with an O_2 equivalence ratio of 1 as a reference, we substituted the quantities of H_2O produced by three aliphatic hydrocarbon functional groups into Eq. (5). The resulting order of H_2O generation rates, from highest to lowest, is: -CH_3 (40%) > -CH (39.69%) > -CH_2 (38.33%). Similarly, substituting the amounts of CO_2 generated by these functional groups into Eq. (6) yields the following order for CO_2 formation rates: $-CH_2$ (53.85%) > $-CH_3$ (53.57%) > −CH (53.16%). Furthermore, when substituting the quantities of CO produced by these aliphatic hydrocarbon functional groups into Eq. (7), we find that the order for CO generation rates is: -CH_3 (30.71%) > -CH (29.47%) > -CH_2 (28.85%). Overall, it can be concluded that among aliphatic hydrocarbon functional groups, $-CH_2$ exhibits the highest tendency for CO_2 conversion while $-CH_3$ demonstrates superior tendencies for both H_2O and CO conversions during combustion. In the whole combustion reaction process, more than 8000 decomposition steps will occur, and the gas phase products will also be transformed into each other. Therefore, the final determined proportion of gas phase products will be obtained by the software 's own post-processing system MD Properties module, which will automatically determine the number of stable gas phase products in the end stage. Although the percentage content of combustion products is very close, it can be approximately considered that it has a corresponding conversion tendency due to its large production base.

The analysis above indicates that CO_2, H_2O, and CO are the predominant Gas-phase products resulting from the combustion of functional groups in coal. Additionally, trace amounts of CH_4 may be generated; however, its formation primarily occurs later in the reaction process, predominantly during the middle to late stages of

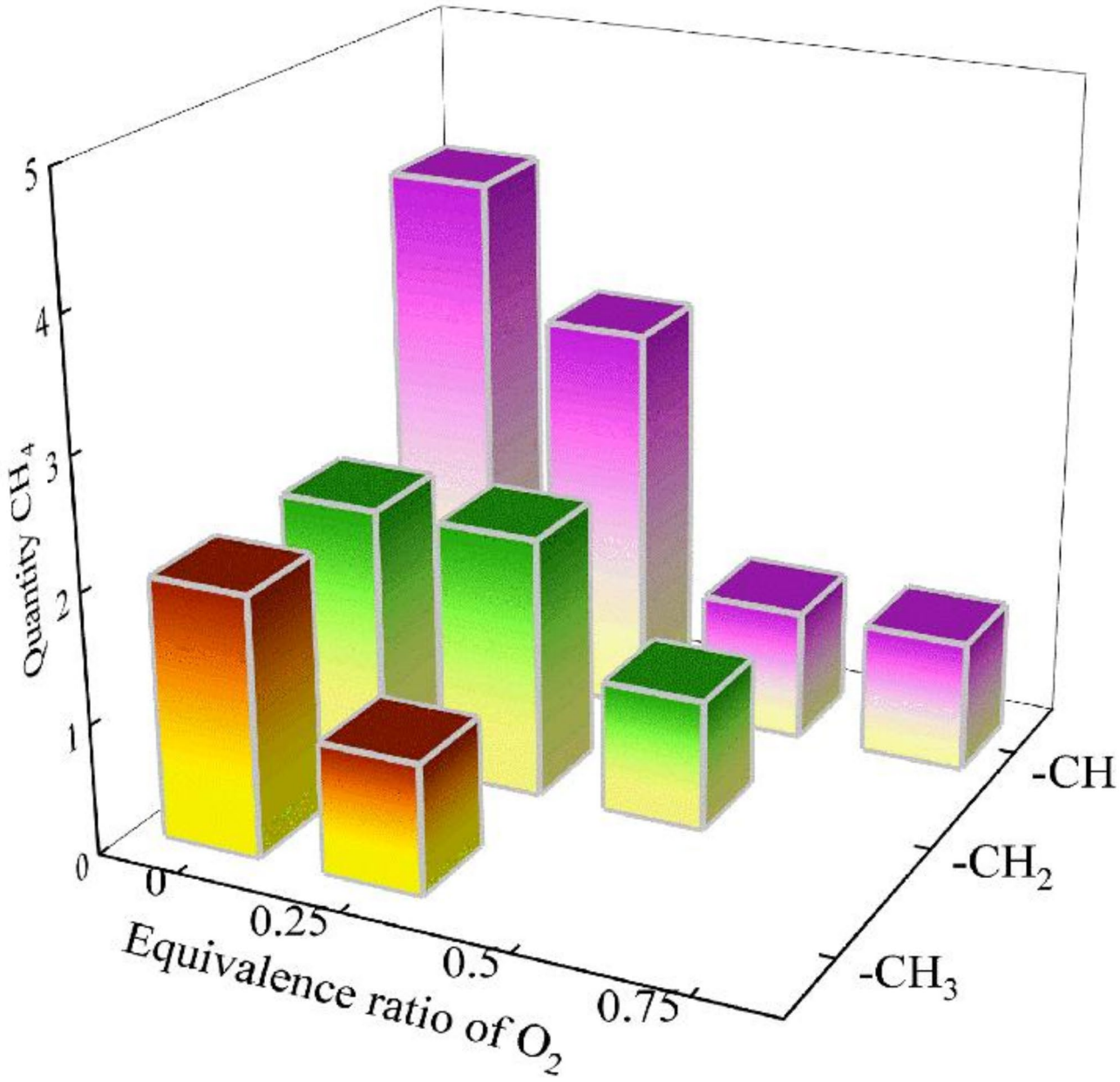

Fig. 7. Analysis of CH_4 production of different functional groups.

Typical chemical equations	
$\cdot H+\cdot CH_2+C_{12}H_{11}=>CH_4+C_{12}H_{10}$	$\cdot H+\cdot CH_3+C_3H_4=>CH_4+C_3H_4$
$\cdot H+\cdot CH_3+C_9H_4O_2=>CH_4+C_9H_4O_2$	$\cdot CH_3+C_3H_3=>CH_4+C_3H_2$
$\cdot H+\cdot H+C_5H_5=>CH_4+C_4H_3$	$\cdot H+CH_3=>CH_4$

Table 3. The chemical equations of typical reaction path of CH_4 formation.

continuous reactions. As shown in Fig. 7, a lower O_2 concentration correlates with increased CH_4 production, suggesting that CH_4 formation is largely influenced by pyrolysis pathways. Furthermore, it is observed that the conversion tendency for −CH groups yields the highest levels of CH_4. As shown in Table 3, the reactants involved in hydrocarbon generation predominantly consist of low-carbon-content small molecular compounds. The reaction is favored under conditions of reduced oxygen content, suggesting that hydrocarbon formation primarily results from the thermal decomposition of carbon-containing small molecules undergoing incomplete combustion in high-temperature environments. Furthermore, the generation of hydrocarbons is significantly

influenced by ·H free radicals. Analysis of typical reaction equations reveals that ·H free radicals are crucial initiators within the hydrocarbon formation pathway, exhibiting a positive correlation with this process. The ·H radical, characterized by an unpaired electron on the hydrogen atom, demonstrates high reactivity and engages with reactants to facilitate hydrogen atom transfer, ultimately leading to product formation. This free radical mechanism is pivotal in organic chemistry and frequently serves as a catalyst for chain reactions and the synthesis of novel organic molecules.

Free radical analysis in the combustion reaction of aliphatic hydrocarbon functional groups

In the combustion reaction system involving three functional groups, a significant quantity of free radicals is generated[36], including ·O free radicals, ·HO free radicals, and ·H free radicals. The typical chemical equations representing the formation pathways of these three types of free radicals are presented in Table 4. From the preceding analysis, it is evident that free radicals serve as crucial initiators for the chemical reactions occurring among various functional groups and their transition products. Investigating the dynamics of free radicals changes within the combustion reaction system of functional groups constitutes an essential aspect of elucidating the mechanisms underlying coal's functional group combustion reactions.

As shown in Fig. 8(a ~ c), the ·O free radical generation curves in functional group reaction systems with varying oxygen content show significant differences. In particular, lower O_2 concentrations correlate with reduced ·O free radical production and an earlier onset of curve flattening. The oxidation activity of different functional groups can be inferred from the time at which their respective ·O free radicals generation curves begin to flatten, with faster flattening indicating a greater propensity for oxidation reactions.

In order to illustrate the behaviour of the reaction system with an equivalence ratio of 1, it is sufficient to consider the time sequence of the ·O radical generation curves in the three functional groups. These tend to be flat, as follows: The order of the functional groups is −CH (approximately 18,000 fs) > $-CH_2$ (approximately 20,000 fs) > $-CH_3$ (approximately 22,000 fs), which is consistent with the experimental results. This pattern is in accordance with the order of the stability of the three functional groups, from the weakest to the strongest. The combustion reaction system obtained in the experiment indicates that the rate of reaction with the ·O radicals is directly proportional to the oxidative activity of the functional group, confirming the stability of the three functional groups under the combustion reaction system from the perspective of the·O radicals. The absence of ·O radicals in the pyrolysis reaction system with an O_2 equivalent ratio of 0 indicates that, in the absence of oxygen, aliphatic hydrocarbon functional groups must undergo decomposition by the oxidation front reaction in order to generate ·O radicals.Consequently, as shown in Table 4, there are three primary pathways for the generation of ·O free radicals. The first pathway involves high-temperature conditions where O_2 molecules absorb energy and undergo thermal cracking to yield two ·O free radicals; this process is exothermic. The second pathway pertains to redox reactions involving electron transfer between oxygen-containing free radicals at elevated temperatures. The third reaction involves the dissociation of oxygen-containing transition products generated from the oxidation of functional groups, leading to the formation of ·O free radicals. This process can be characterized by the cleavage of intramolecular O–O bonds, which is an endothermic reaction.

The ·O free radical	The·HO free radical	The·H free radical
$C_{19}H_{14}O_2$=>·O + $C_{19}H_{14}O$	·O + $C_{19}H_{12}O_5$=>·HO + $C_{19}H_{11}O_5$	$C_{19}H_{16}$=>·H + $C_{19}H_{15}$
$C_{18}H_8O_{10}$=>·O + $C_{18}H_8O_9$	·O + $C_{18}H_9O_3$=>·HO + $C_{18}H_8O_3$	$C_{18}H_{14}$=>·H + $C_{18}H_{13}$
$C_{17}H_{11}O_8$=>·O + $C_{17}H_{11}O_7$	·O + $C_{17}H_{10}O_7$=>·HO + $C_{17}H_9O_7$	$C_{17}H_{13}$=>·H + $C_{17}H_{12}$
$C_{16}H_9O_9$=>·O + $C_{16}H_9O_8$	·O + $C_{16}H_8O_{10}$=>·HO + $C_{16}H_7O_{10}$	$C_{16}H_{15}$=>·H + $C_{16}H_{14}$
$C_{15}H_8O_7$=>·O + $C_{15}H_8O_6$	·O + $C_{15}H_8O_6$=>·HO + $C_{15}H_7O_6$	$C_{15}H_{11}$=>·H + $C_{15}H_{10}$
$C_{14}H_5O_6$=>·O + $C_{14}H_5O_5$	·O + $C_{14}H_{11}O_2$=>·HO + $C_{14}H_{10}O_2$	$C_{14}H_{14}$=>·H+·H + $C_{14}H_{12}$
$C_{13}H_7O_5$=>·O + $C_{13}H_7O_4$	·O + $C_{13}H_7O_9$=>·HO + $C_2H_2O_3$ + $C_{11}H_4O_6$	$C_{13}H_{12}$=>·H + $C_{13}H_{11}$
$C_{12}H_7O_6$=>·O + $C_{12}H_7O_5$	·O + $C_{12}H_7O_5$=>·HO + $C_{12}H_6O_5$	$C_{12}H_{10}$=>·H+·H + $C_{12}H_8$
$C_{11}H_4O_6$=>·O + $C_{11}H_4O_5$	·O + $C_{11}H_5O_5$=>·HO + $C_{11}H_4O_5$	$C_{11}H_8$=>·H + $C_{11}H_7$
$C_{10}H_6O_4$=>·O + $C_{10}H_6O_3$	·O + $C_{10}H_5O_5$=>·HO + $C_{10}H_4O_5$	$C_{10}H_7$=>·H + $C_{10}H_6$
$C_9H_4O_6$=>·O + $C_9H_4O_5$	·O + $C_9H_5O_6$=>·HO + $C_9H_4O_6$	C_9H_9=>·H + C_2H_3 + C_7H_5
$C_8H_3O_7$=>·O+·CHO + $C_7H_2O_5$	·O + $C_8H_3O_2$=>·HO + $C_8H_2O_2$	C_8H_6=>·H + C_8H_5
$C_7H_6O_4$=>·O + $C_7H_6O_3$	·H + $C_7H_4O_6$=>·HO + $C_7H_4O_5$	C_7H_8=>·H + C_7H_7
$C_6H_5O_2$=>·O + C_6H_5O	·H + $C_6H_3O_5$=>·HO + $C_6H_3O_4$	C_6H_6O=>·H + C_6H_5O
$C_5H_3O_4$=>·O + $C_5H_3O_3$	·H + C_5H4O6=>·HO + $C_5H_4O_5$	$C_5H_5O_2$=>·H + $C_5H_4O_2$
$C_4H_3O_4$=>·H+·O + $C_4H_2O_3$	·H + C_4HO_5=>·HO + C_4HO_4	$C_4H_2O_3$=>·H + C_4HO_3
C_3HO_4=>·O + C_3HO_3	·H + C_3HO_3=>·HO + C_3HO_2	C_3H_2O=>·H + C_3HO
C_2O_3=>·O + C_2O_2	·H+·H + $C_2H_2O_3$=>·HO + $C_2H_3O_2$	$C_2H_2O_2$=>·H + C_2HO_2
CH_2O_3=>·O+·CH_2O_2	·H + CHO_4=>·HO + CHO_3	CH_2O_3=>·H + CHO_3
·HO+·HO_2=>·O + H_2O_2	·H+·O=>·HO	O_2 + H_2O=>·H + HO_3
O_2=>·O+·O		·HO=>·H+·O

Table 4. Typical chemical equations of free radical formation reaction path.

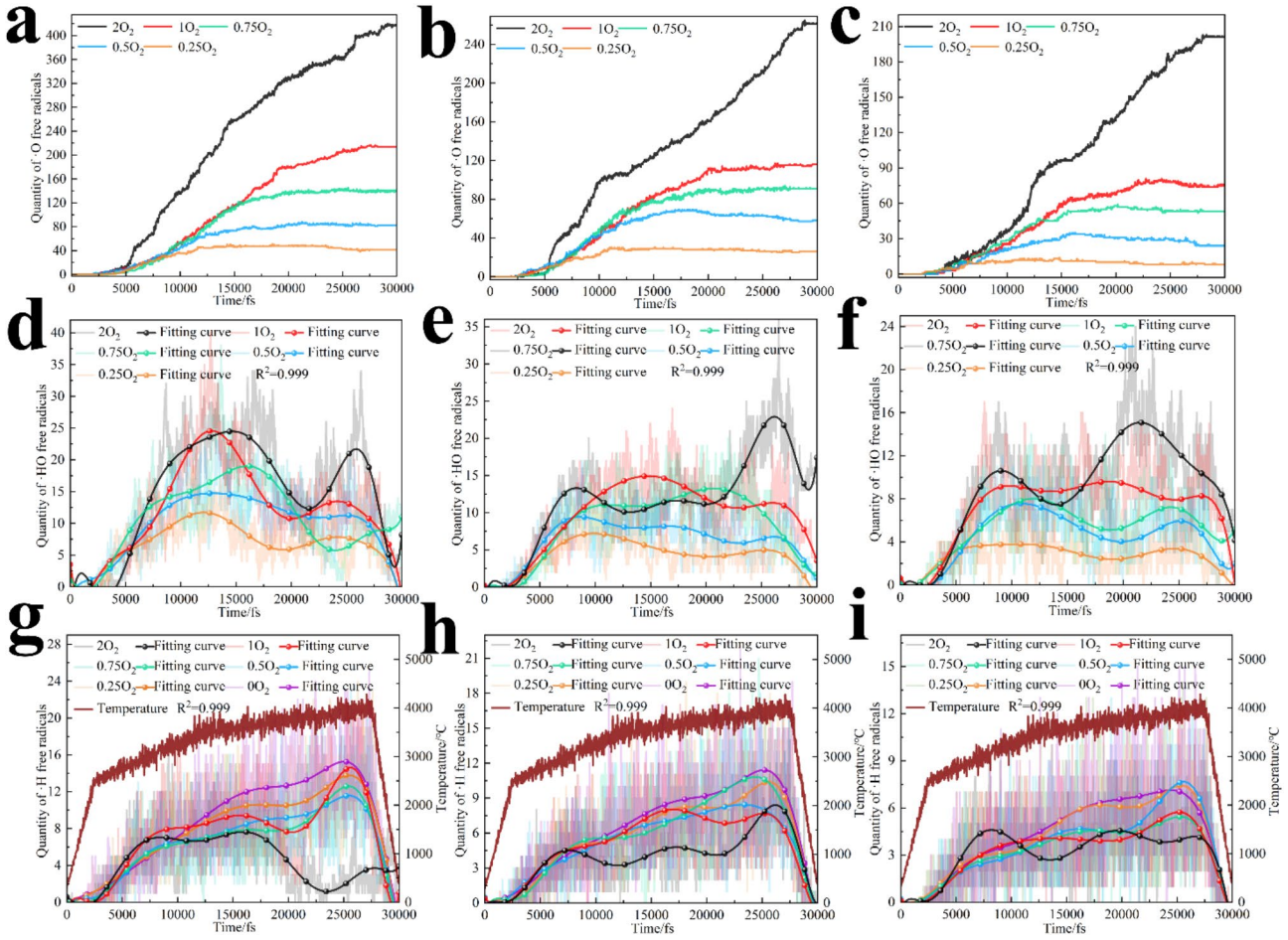

Fig. 8. Free radical analysis of combustion reaction of different functional groups. (**a**) ·O free radical production of -CH; (**b**) $-CH_2$; (**c**) $-CH_3$. (**d**) ·HO free radical production of -CH; (**e**) $-CH_2$; (**f**) $-CH_3$. (**g**) ·H free radical production of -CH; (**j**) $-CH_2$; (**i**) $-CH_3$.

As shown in Fig. 8(d ~ f), the quantity of ·HO free radicals that can be captured within the combustion reaction system of aliphatic hydrocarbon functional groups is relatively low, and there exists significant fluctuation in the generation curve of ·HO free radicals over short time intervals. To enhance analytical efficiency, polynomial fitting has been applied to the ·HO free radical generation curves across three distinct functional group combustion reaction systems under varying oxygen concentrations. The pronounced fluctuations observed in these curves suggest that the ·HO free radicals produced during combustion are more likely to be converted into other products, such as H_2O, rather than forming stable ·HO free radicals. Additionally, factors such as temperature, spatial configuration, and oxygen concentration exert considerable influence on the functional group combustion reaction system; even minor variations can significantly impact both reaction rates and product formation, leading to substantial fluctuations in the generated ·HO free radical curves. Furthermore, the structural characteristics and properties of the various functional groups may contribute to differences in their reactivity and the resulting products, thereby influencing the yield and volatility of ·HO free radicals. The temporal variation of ·HO free radicals across the three functional groups is not significantly affected by temperature; rather, it is primarily associated with the oxygen content within the system. It is noteworthy that this temporal variation exhibits a degree of consistency. Higher oxygen concentrations correlate with an increased generation of ·HO free radicals and greater fluctuations in their concentration over time. As illustrated in Table 3, the primary pathway for the generation of aliphatic hydrocarbon functional group ·HO free radicals entails redox reactions between ·O free radicals, ·H free radicals, and carbon-containing compounds. In this context, the ·O free radical functions as an oxidant, participating in exothermic redox processes.

As shown in Fig. 8 (g ~ i), the quantity of ·H free radicals that can be captured within the combustion reaction system of aliphatic hydrocarbon functional groups is relatively low. Consequently, polynomial fitting is performed using the same methodology applied to the ·HO free radical generation curve. The resulting curve exhibits significant fluctuations, indicating that the production of ·H free radicals occurs with considerable variability over short time intervals. This suggests that ·H free radicals generated by functional groups during combustion reactions are less stable and tend to convert into other combustion products rather than forming stable ·H free radicals. Furthermore, as the temperature increases, the fluctuation range of ·H free radical generation exhibits a gradual escalation, with the upward trend of the fitting curve mirroring that of the

temperature rise in the functional group combustion reaction system. This observation highlights the significant influence of temperature on ·H free radical generation. The impact of temperature variations on the reaction rate and equilibrium position consequently affects the production of ·H free radicals. consequently, competitive reactions within the functional group combustion pathway can yield a range of intermediate products and by-products, which contribute to substantial variability in ·H free radical output. The generation curves of ·H free radicals in the combustion reaction systems of three aliphatic hydrocarbon functional groups under varying oxygen concentrations exhibit notable consistency. Specifically, an increase in oxygen content correlates with a decrease in ·H free radicals production. This phenomenon can be attributed to the nature of functional group combustion as a redox process, whereby both an oxidant and a reducing agent are involved. In these combustion systems, oxygen typically serves as the oxidant, while organic matter acts as the reducing agent. In addition, the combustion of coal is also affected by the trace load of its internal transition metal oxides, so it also has a certain catalytic effect. An increase in oxygen content is associated with a higher concentration of O_2 as an oxidant. The enhanced oxidative capacity of oxygen facilitates the oxidation of ·H free radicals within organic matter to H2O, thereby reducing the concentration of ·H free radicals. Furthermore, elevated oxygen levels facilitate more complete combustion of organic matter, resulting in greater production of CO_2 and H_2O while simultaneously reducing the generation of ·H free radicals.As illustrated in Table 3, aliphatic hydrocarbon functional groups can undergo a preliminary reaction pathway that culminates in the generation of ·H free radicals. The formation of ·H free radicals occurs as a consequence of the cracking reactions of these functional groups, resulting in the generation of both ·H free radicals and an excess of carbon-containing fragments as by-products. This process entails the cleavage of the original chemical bonds, which results in the release of energy. Consequently, the generation of ·H free radicals is characterised as an exothermic reaction. Concurrently, the formation of specific ·H free radicals occurs via the oxidation of H_2O and the dissociation of ·HO free radicals, both of which are exothermic reactions.

Conclusions

This paper presents an investigation into the reaction paths, gas-phase products and free radicals of combustion and pyrolysis of three aliphatic hydrocarbon functional groups, based on the ML potential MD method in AMS-2024 software.The rationality of the ML potential MD model was validated through the utilisation of TG-FTIR and in-situ FTIR experimentation. The experimental and simulation results demonstrate that the stability of the three aliphatic hydrocarbon functional groups within the combustion reaction system is in the following order of weakness to strength: The order of the aliphatic hydrocarbon functional groups is thus $-CH_3 > -CH_2 > -CH$; the order of the gas-phase products is $H_2O > CO_2 > CO > CH_4$. The -CH functional group exhibits the highest propensity for converting methane, the $-CH_2$ group displays the highest propensity for converting CO_2 dioxide (53.85%), and the $-CH_3$ group exhibits the highest propensity for converting H_2O (40%) and CO (30.71%) monoxide. The combustion reaction process of aliphatic hydrocarbon functional groups can be divided into four main stages: a reaction pre-stage, an oxidation and combustion reaction stage, a continuous reaction stage and a reaction completion stage. The gas-phase products are primarily generated during the oxidation and combustion reaction stage and in significant quantities during the continuous reaction stage. The oxidative combustion process of aliphatic hydrocarbon functional groups is exothermic, and in the anaerobic pyrolysis reaction system it is absorptive. As the oxygen content decreases, the system exhibits a stronger tendency to transition from exothermic to absorptive in the late stage of the reaction. This implies that as the oxygen content decreases, the pyrolysis parallel reaction of the functional groups intensifies. The dehydrogenation effect brought about by the pyrolysis parallel reaction provides carbonaceous fragments and a plethora of free radicals, which serve to accelerate the subsequent oxidation reaction of functional groups. Meanwhile, the peroxides and complexes generated by the oxidation and dehydrogenation reaction of functional groups cause the accumulation of heat and promote the further occurrence of the pyrolysis reaction. These processes are complementary and occur in parallel. Free radicals play a significant role in numerous radical reactions within the system. Among these, the ·O free radical plays an important role as a fluxing agent in the oxidative combustion of functional groups, while the ·HO radical and the ·H free radical are significant initiators in the oxidative combustion of functional groups. The change of the ·O free radical exerts a significant influence on the generation path of CO_2 and CO. The ·O free radical exhibits a positive correlation with the generation of CO_2 and a negative correlation with the generation of CO. The change of the ·HO free radical exerts a substantial influence on the generation path of H_2O, and the two have a positive correlation. The change of the ·H free radical exerts a considerable influence on the generation path of CH_4, and the two have a positive correlation. The results can provide theoretical support for the study of carbon emission inhibition from the perspective of functional groups, and also provide a new idea for the research and development of inhibitors. In future studies, HO_2 radicals normally plan an important role in the low-T oxidation cycle.

Data availability

Data is provided within the manuscript or supplementary information files.

Received: 6 October 2024; Accepted: 29 January 2025
Published online: 24 March 2025

References

1. Cheng, Y. P. & Pan, Z. J. Reservoir properties of Chinese tectonic coal: a review. *Fuel* . **260**(15), 1–22 (2020).
2. Jia, J. J. et al. Adsorption of $CH_4/CO_2/N_2$ by different functional groups in coal. *Fuel* . 335 (2023).
3. Wang, K. et al. Comparison of combustion characteristics and kinetics of jurassic and carboniferous-Permian coals in China[J]. *Energy*. **254**, 124315 (2022).

4. Xu, T. et al. Heat Effect of Oxidation of Aliphatic Hydrocarbon groups on the Piecewise characteristics and spontaneous Combustion tendency of coal. *Solid Fuel Chem.* **55**(5), 338–347 (2021).
5. Allena, O. S. et al. Can energy sector reach carbon neutrality with biomass limitations? *Energy*. 249 (2022).
6. Wei, Y. M. et al. Policy and management of Carbon Peaking and Carbon Neutrality. *Literature Rev. Eng.* **14**, 5263 (2022).
7. Li, J. et al. Thermodynamics of oxygen-containing intermediates and their role in coal spontaneous combustion. *Energy*. **260**, 124989 (2022).
8. Zhang, Y. et al. Analysis of oxidation pathways for characteristic groups in coal spontaneous combustion. *Energy* **254**, 124211 (2022).
9. Chao, J. K. et al. Oxidation and spontaneous combustion characteristics of particulate coal under stress–heat–gas interactions. *Science of the Total Environment*. **947**, 174567 (2024).
10. Duan, Z. X. et al. The promotion mechanism of persistent free radicals on low-temperature oxidation of coal. *Fuel*. **376**, 132698 (2024).
11. Tao, Y. D. et al. Study on the Effect of Oxygen on Free Radical Generation in Coal[J]. *Combust. Sci. Technol.* **196**(7), 943–960 (2024).
12. Liu, Y. et al. Research Status and Development Trend of coal spontaneous Combustion Fire and Prevention Technology in China: a Review. *ACS omega*. **9**(20), 21727–21750 (2024).
13. Zhang, X. et al. Influence of mudstone on coal spontaneous combustion characteristics and oxidation kinetics analysis[J]. *Sci. Rep.* **14**(1), 9744–9744 (2024).
14. Chen, L. Z. et al. Reaction pathways and cyclic chain model of free radicals during coal spontaneous combustion. *Fuel*. **293** (2021).
15. Zhang, X. et al. Study on the kinetics of chemical structure reaction in coal catalyzed by OH free radicals. *Energy*. **285** (2023).
16. Yan, G. Z. et al. Exploring carbon dioxide generation in combustion of long-flame coal in huating mining area by using ReaxFF MD. *Case Studies in Thermal Engineering*. **55**, 104171 (2024).
17. Zhang, Y. X. et al. Reaction mechanism and kinetics of kerogen dehydrogenation and cyclization investigated by density functional theory. *Fuel*. **371**, (2024).
18. Han, D. D. et al. Exploration and Frontier of coal spontaneous Combustion Fire Prevention materials. Processes. **12**(6), 1155 (2024).
19. Yu, Z. Y. et al. In-situ infrared and kinetic characteristics analysis on pyrolysis of tar-rich coal and macerals. *Fuel*. **348** (2023).
20. Chi, C. & Ping, S. O. A universal graph deep learning interatomic potential for the periodic table. *Nat. Comput. Sci.* **2** (11), 718–728 (2022).
21. Liu, H. et al. Effects of oxidation on physical and chemical structure of a low rank sub-bituminous coal during the spontaneous combustion latency. *Energy*. **272**, (2023).
22. Zhang, Y. L. et al. Kinetic study on changes in methyl and methylene groups during low-temperature oxidation of coal via in-situ FTIR. *Int. J. Coal Geol.* **154-155**, 155-164 (2016).
23. Bai, Z. J. et al. Mechanism of [BMIM][BF_4] inhibiting coal groups activity from experiments and DFT calculations. *Fuel*. **353**. (2023).
24. Zhang, W. et al. Highly effective flame-retardant coatings consisting of urea-formaldehyde resin/aluminium hydroxide/boric acid for polystyrene foam: Properties and mechanisms investigation. Progress in Organic Coatings. **196**, 108766 (2024).
25. Kwon, H., Shabnam, S. & Duin, V. C. Numerical simulations of yield-based sooting tendencies of aromatic fuels using reax FF molecular dynamics. *Fuel* **262**, 116545 (2020).
26. Yu, M. G. et al. Reactive force field molecular dynamics (ReaxFF-MD) simulation of lignite combustion under an external electric field. *Fuel*. **358**(PA) (2024).
27. Russo, F. M. & Duin, V. C. A.Atomistic-scale simulations of chemical reactions: bridging from quantum chemistry to engineering. *Nuclear Inst. Methods Phys. Res. B*. **269**(14), 1549–1554 (2011).
28. Qiu, Y. et al. Reactive force field molecular dynamics (ReaxFF MD) simulation of coal oxy-fuel combustion. *Powder Technol.*, **361**, 337–361348 (2020).
29. Jia, J. Z. et al. Molecular structure characterization analysis and molecular model construction of anthracite. *PloS One*. **17**(9), e0275108–e0275108 (2022).
30. Shaheed, R., Mohammadian, A. & Gildeh, H. K. A comparison of standard k–ε and realizable k–ε turbulence models in curved and confluent channels. *Environ. Fluid Mech.* **19**(2) (2019).
31. Gong, Z. J., Wang, K. X. & Wu, W. P. Study of coal pyrolysis characteristics based on the TG-FTIR technology. *J. Inner Mongolia Univ. Sci. Technol.* **35**(03), 247–251 (2016).
32. Qi, X. Y. et al. In situ FTIR study on real-time changes of active groups during lignite reaction under low oxygen concentration conditions. *Energy Inst.* **92** (5), 1557–1566 (2019).
33. Xu, D. X. et al. The generation mechanism of CO and CO_2 in coal spontaneous combustion by mathematical statistical and other methods. *Fuel*. **350** (2023).
34. Meng, L. L. et al. Exploring depolymerization mechanism and complex reaction networks of aromatic structures in chemical looping combustion via ReaxFF MD simulations. *Journal of the Energy Institute*. **107** (2023).
35. Altarawneh, M., Oluwoye, I. & Dlugogorski Z B.Singlet-diradical character in large PAHs triggers spontaneous-ignition of coal. *Combustion and Flame*. **212**, 279-281 (2020).
36. Altarawneh, M. et al. Structural properties of alumina surfaces and their roles in the synthesis of environmentally persistent free radicals (EPFRs). *Nanatechnol. Reviews*, **12**(1), (2023). https://doi.org/10.1515/ntrev-2022-0536

Acknowledgements

This research is conducted with financial support from the National Natural Science Foundation of China (No.52174183 and 52374203).

Author contributions

Jinzhang Jia: Conceptualization, Data curation, Funding acquisition, Investigation, Methodology, Validation, and Writing—original draft. Yumo Wu: Conceptualization, Data curation, Formal analysis, Investigation, Methodology, Software, Visualization, and Writing—original draft. Dan Zhao: Investigation, Software, and Writing—original draft. Fengxiao Wang: Writing – review & editing.Dongming Wang: Validation. Qiang Yang: Software. Yinghuan Xing: VisualizationAll authors reviewed the manuscript.

Declarations

Competing interests

The authors declare no competing interests.

Additional information

Supplementary Information The online version contains supplementary material available at https://doi.org/10.1038/s41598-025-88563-7.

Correspondence and requests for materials should be addressed to Y.W.

Reprints and permissions information is available at www.nature.com/reprints.

Publisher's note Springer Nature remains neutral with regard to jurisdictional claims in published maps and institutional affiliations.